

Effect of irradiation on microstructure of oxide films formed on highly irradiated stainless steel surfaces in PWR

Jiixin Chen¹, Anders Jenssen¹, Fredrik Lindberg², Elena Calota³, Peter Ekström³ and Pål Efsing⁴

¹Studsvik Nuclear AB, SE-611 82 Nyköping, Sweden

²Swerea KIMAB AB, Isafjordsgatan 28 A, SE-164 40 Kista, Sweden

³Swedish Radiation Safety Authority, Solna Strandväg 96, SE-171 16 Stockholm, Sweden

⁴Ringhals AB, SE-430 22 Väröbacka, Sweden

Outline

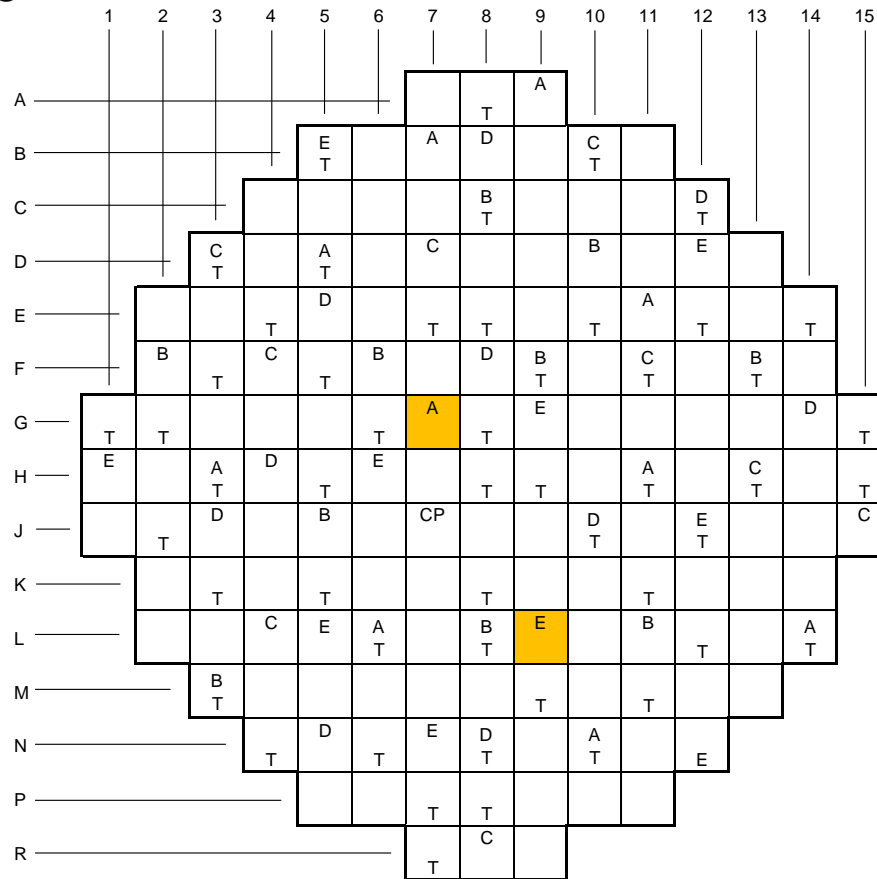
- Background and objective
- Experimental
- Results
- Conclusion

Background

- Irradiation induced material property changes
- Degradation of corrosion resistance?
- Flux thimble tubes

Flux thimble tubes (FTT)

316 type SS

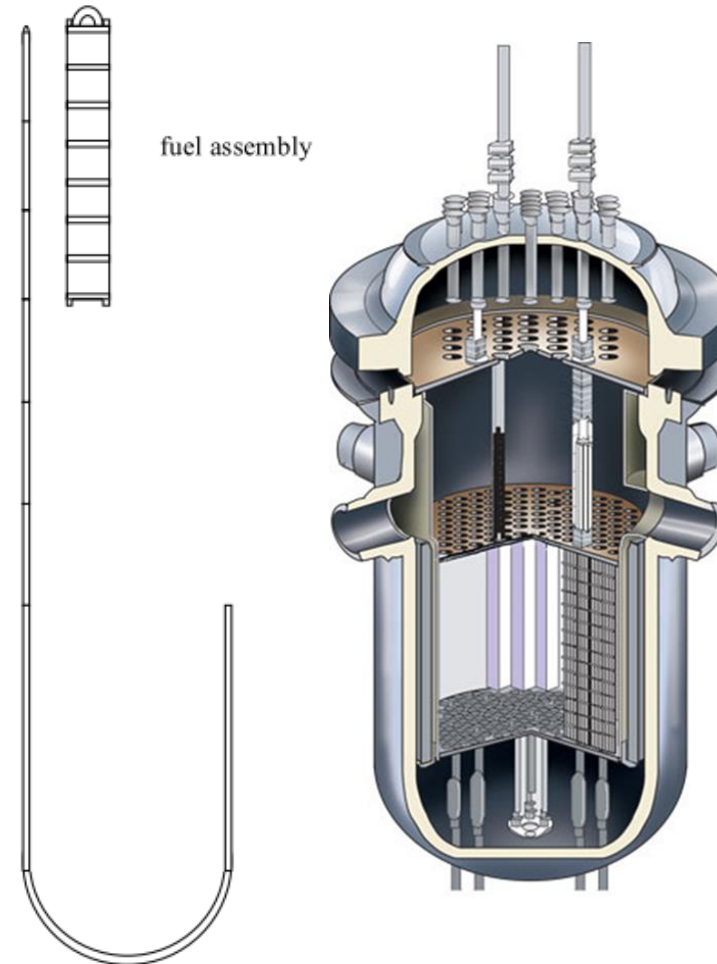


A - Flux Thimble Detector A
 B - Flux Thimble Detector B
 C - Flux Thimble Detector C
 D - Flux Thimble Detector D

E - Flux Thimble Detector E
 CP - Calibration Flux Thimble (common path)
 T - Thermocouple

76 dpa; G7

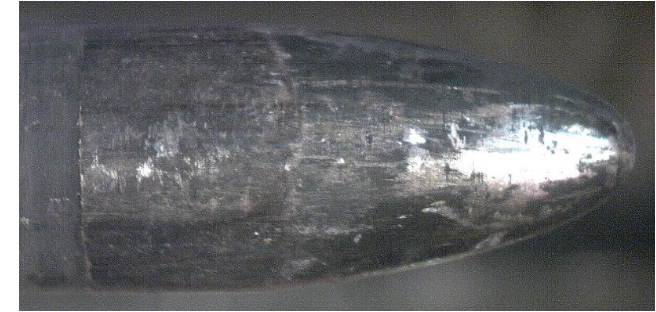
100 dpa; L9



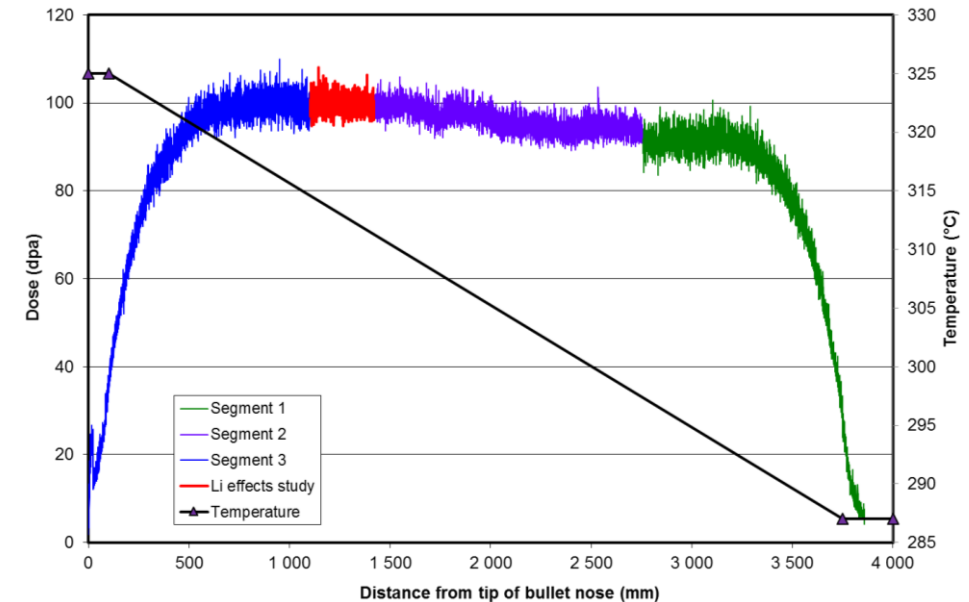
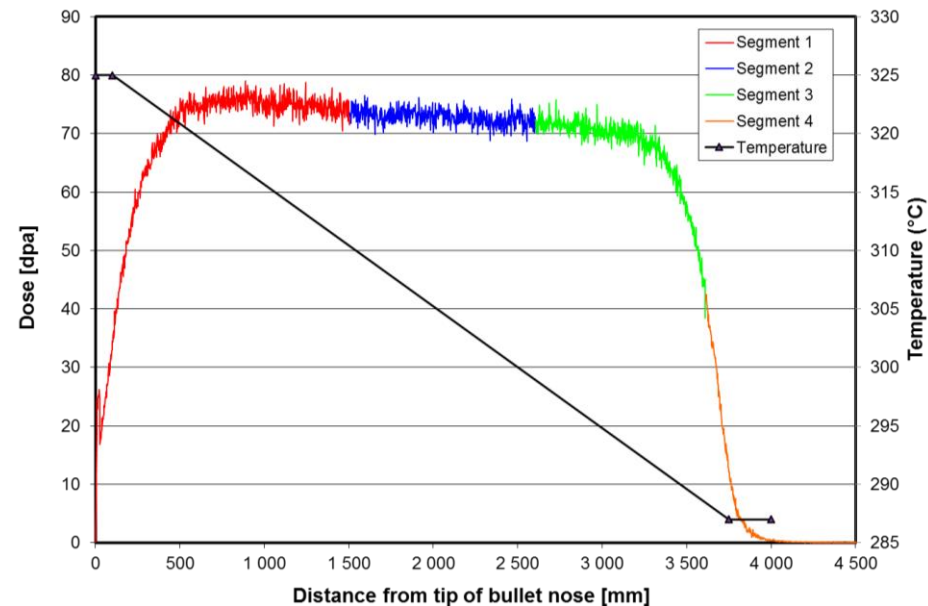
Ringhals unit 2

Flux Thimble Tube

- Cold drawn (~15%) 316 SS: OD 7.62 mm, ID 5.1 mm
- In service for up to 34 reactor cycles w/ max dose >100 dpa
- Temperature: 287 (core inlet) to 325 °C (core outlet)
- Specified unirradiated YS: 483 to 621 MPa



Solid end plug (bullet nose)
at core outlet



Objective

To examine and compare the oxide film microstructures formed at different levels of dose and to look for any evidence of irradiation enhanced corrosion.

Materials examined

Chemical compositions of the austenite stainless steel 316 type material.

C	Si	Mn	P	S	Cr	Ni	Mo	Co	Fe
0.045	0.43	1.7	0.026	0.01	17.4	13.3	2.69	0.04	Balanced

Irradiation doses and temperatures of the examined samples.

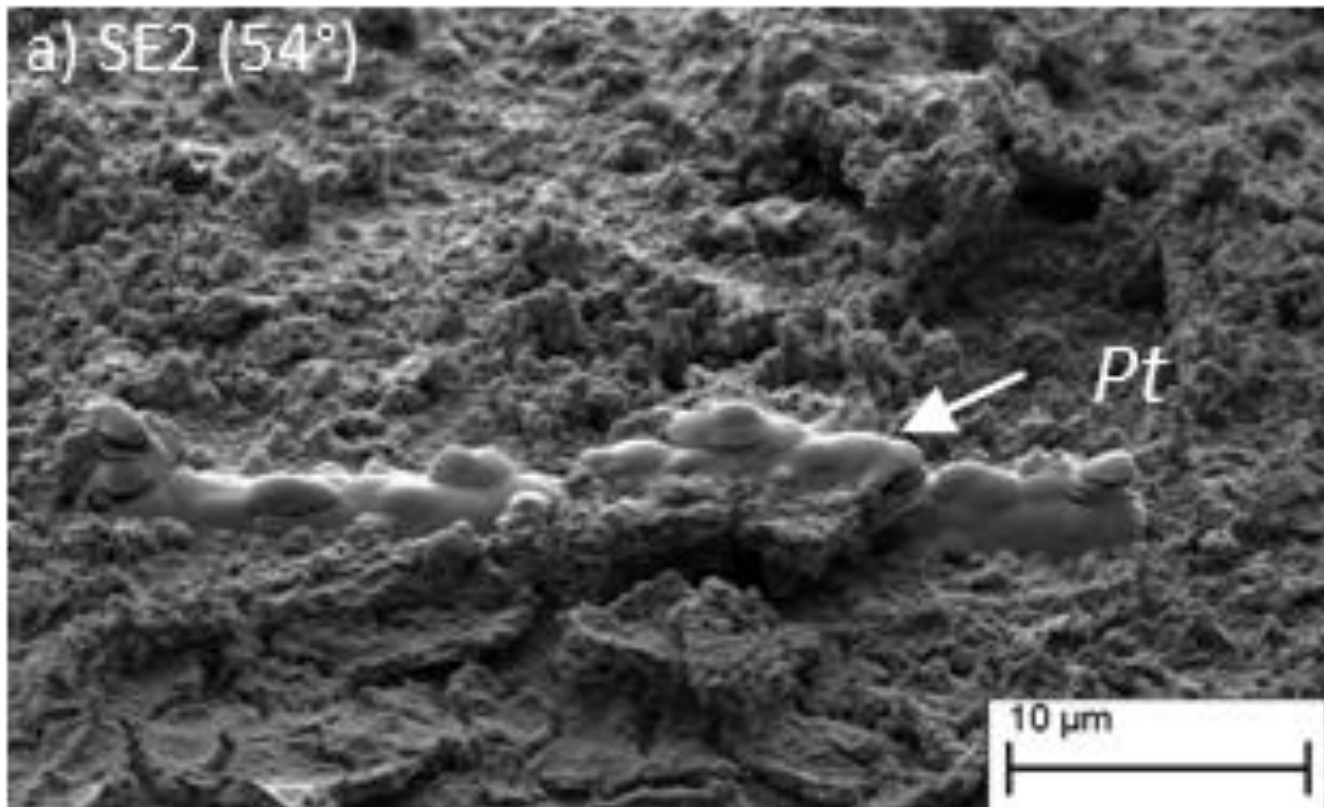
Sample ID	Irradiation dose (dpa)	Coolant temperature (°C)
"dpa_0"	0	287
"dpa_50"	50	315
"dpa_100"	100	315

Electron microscopy

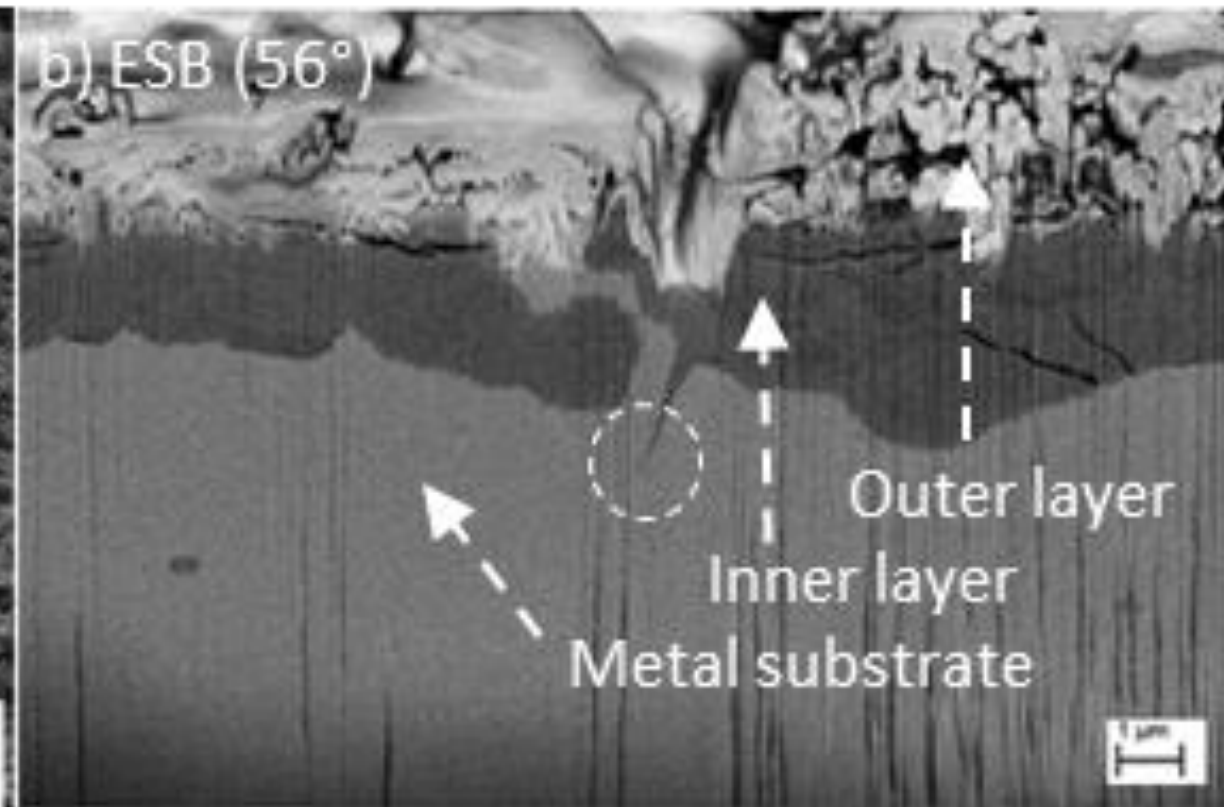
- FIB/SEM (Zeiss Auriga Cross-Beam)
- TEM (JEOL, model JEM 2100F)
 - EDS detectors (Oxford Instruments – X-Max^N 80 TLE)
 - Electron diffraction

Results

Oxide film morphology (0 dpa)



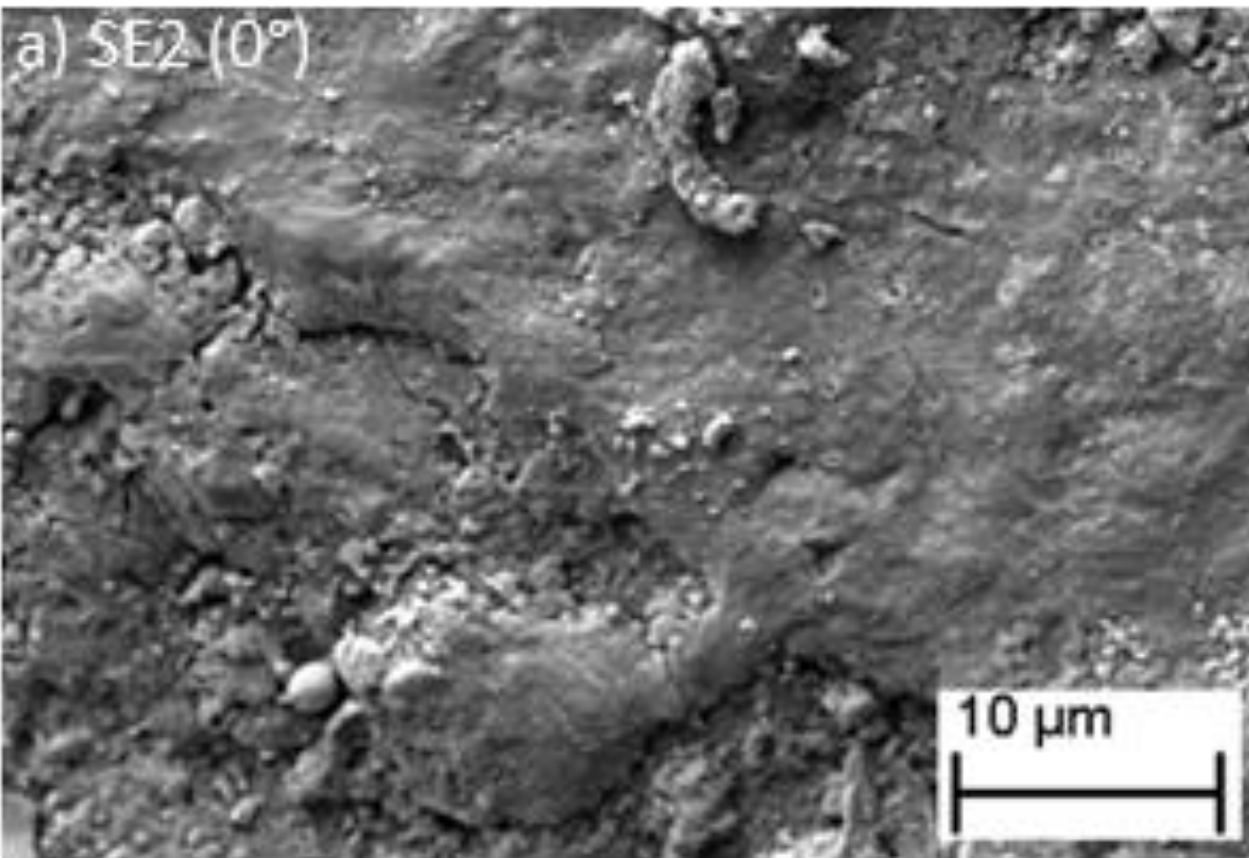
Corroded surface



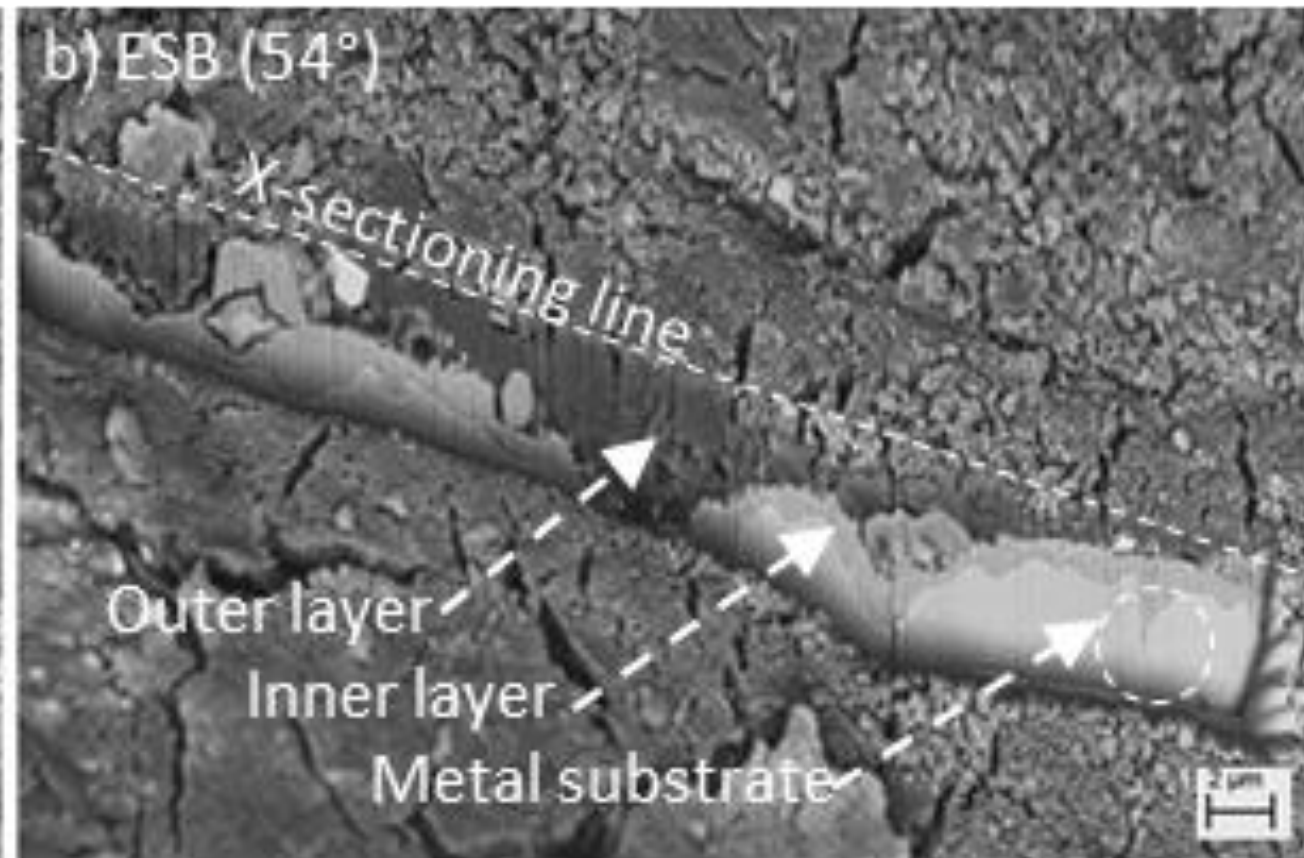
Cross section

Results

Oxide film morphology (50 dpa)



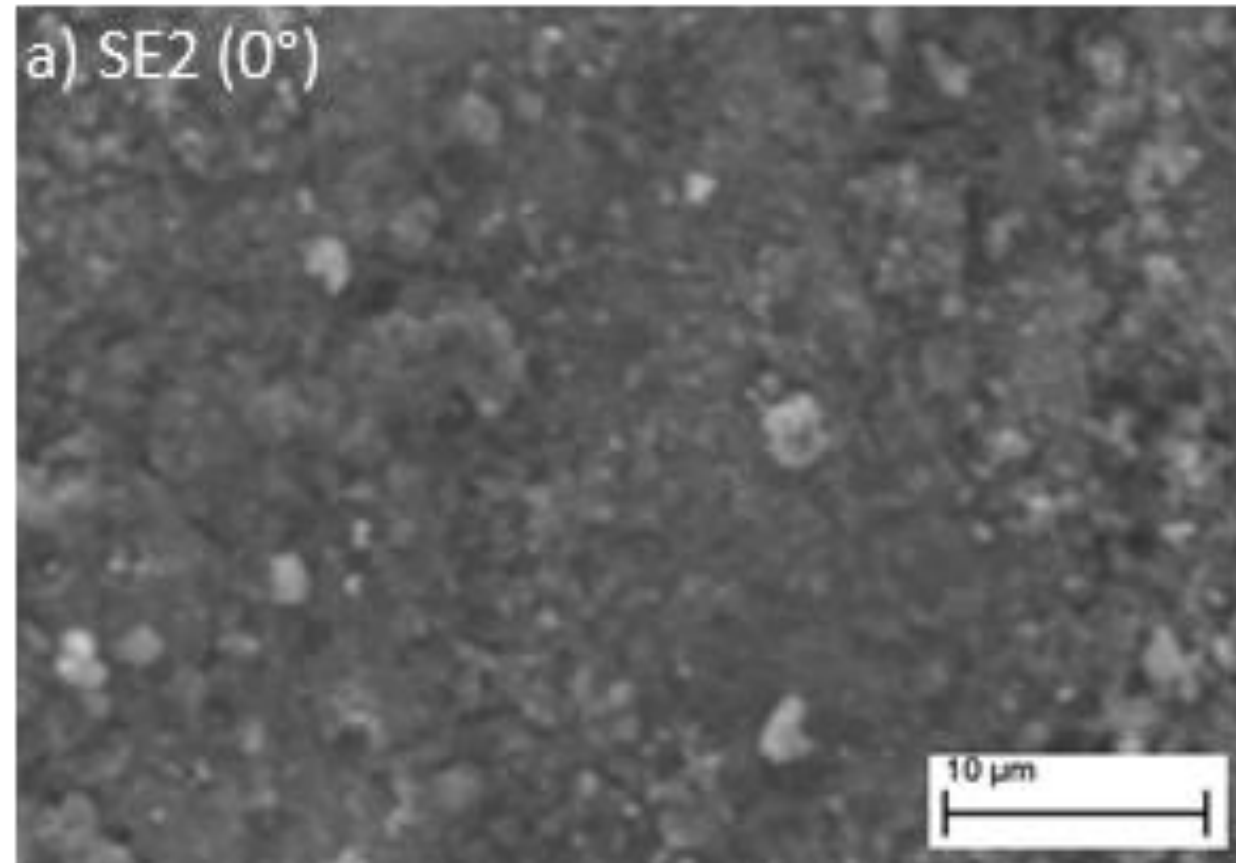
Corroded surface



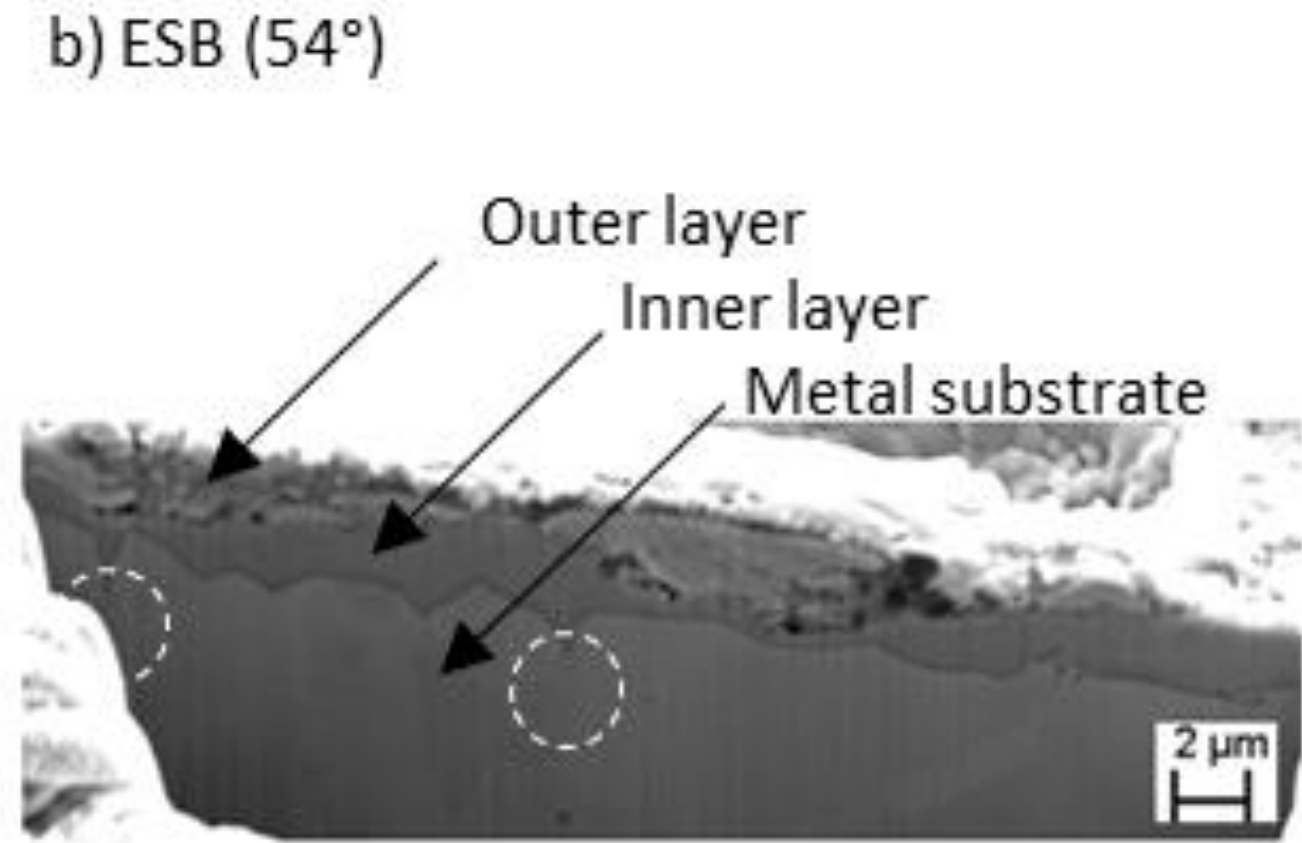
Cross section

Results

Oxide film morphology (100 dpa)



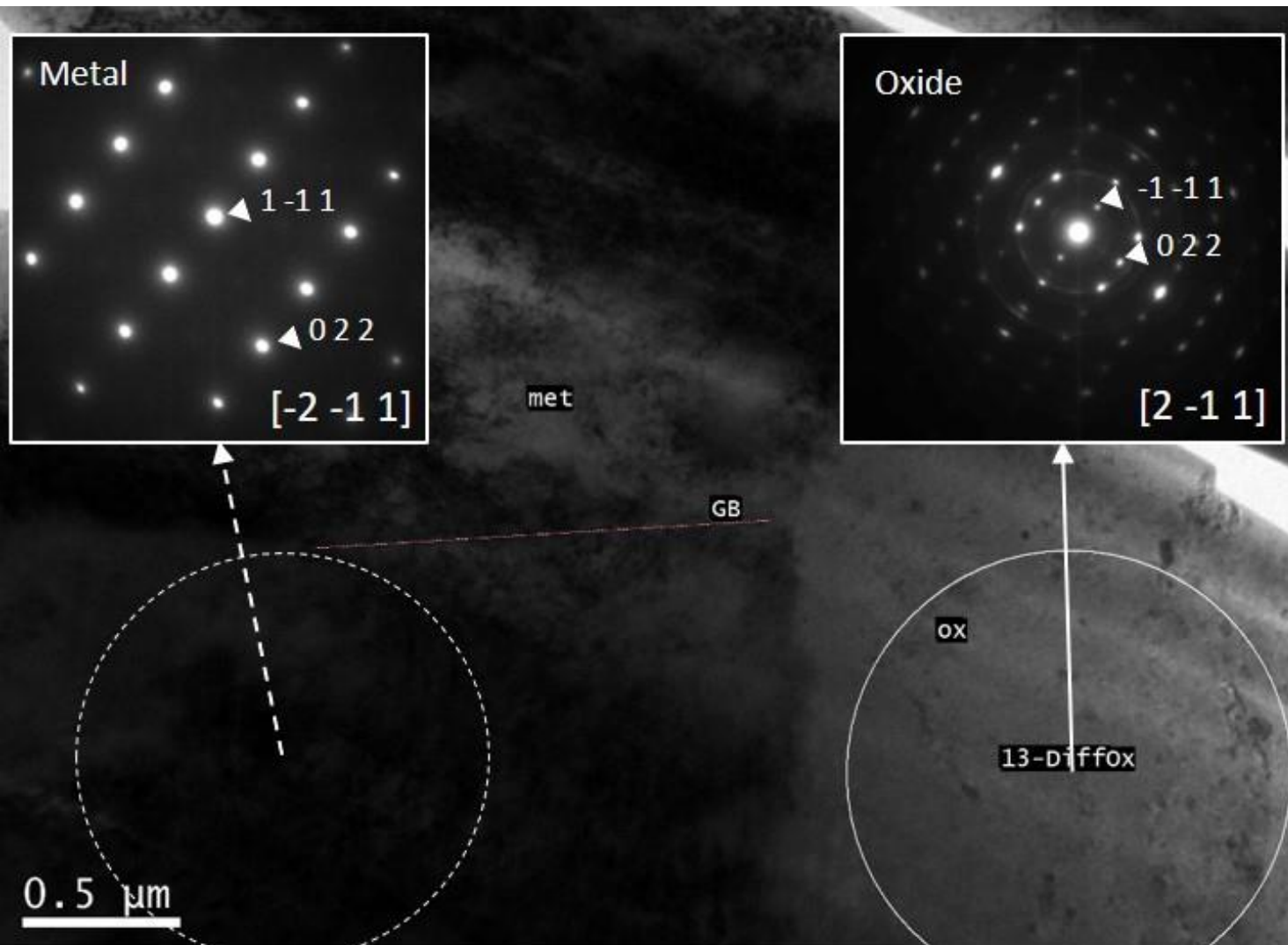
Corroded surface



Cross section

Results

Compositions and crystal structures (0 dpa)



Outer layer

$\text{Ni}_{0.8}\text{Fe}_{1.5}\text{Cr}_{0.7}\text{O}_4$ grains

Inner layer

$\text{Ni}_{0.5}\text{FeCr}_{1.5}\text{O}_4$

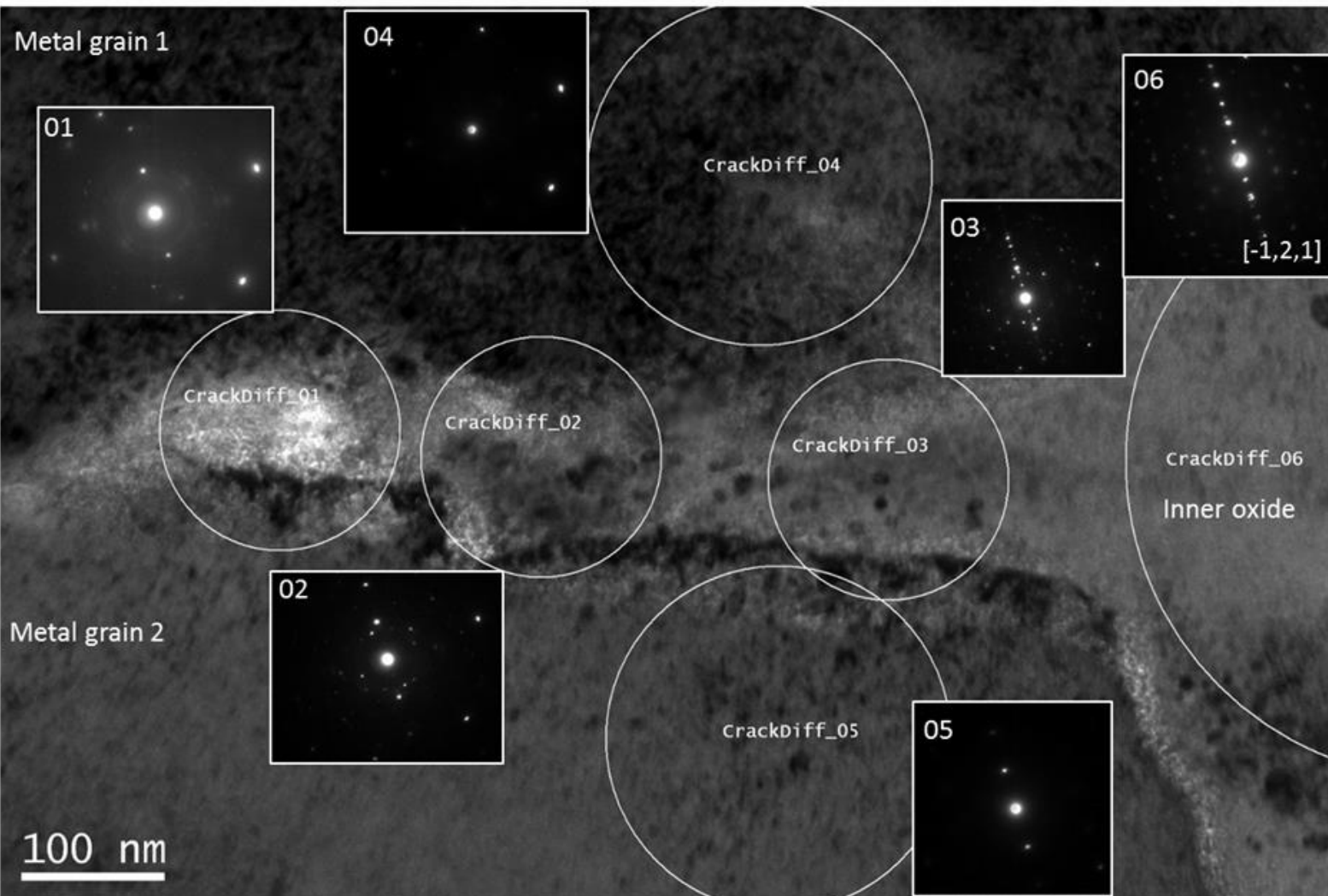
Epitaxial

Metal substrate

FCC austenite

Results

Compositions and crystal structures (50 dpa)



Outer layer

$\text{Ni}_{0.6}\text{Fe}_{1.6}\text{Cr}_{0.7}\text{O}_4$ grains

Inner layer

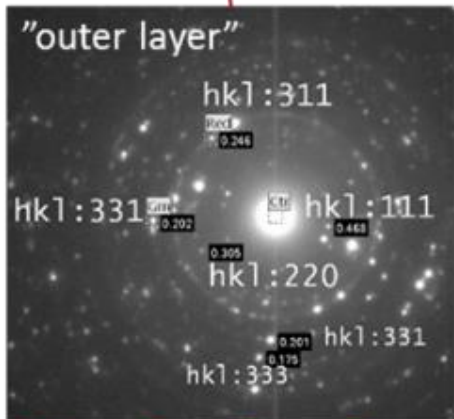
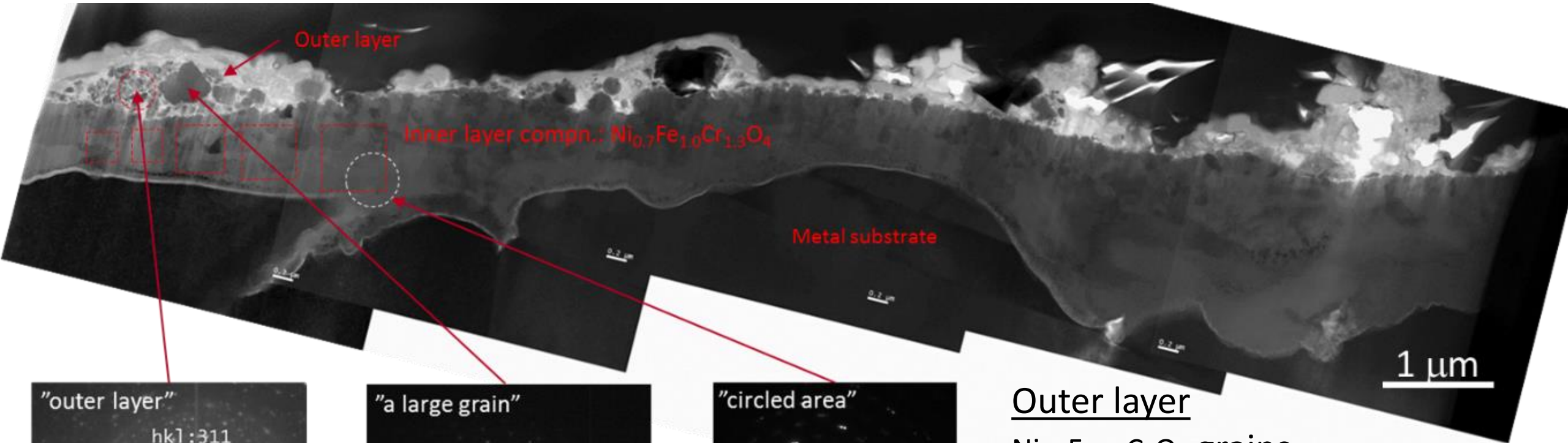
$\text{Ni}_{0.7}\text{Fe}_{1.1}\text{Cr}_{1.2}\text{O}_4$
Epitaxial

Metal substrate

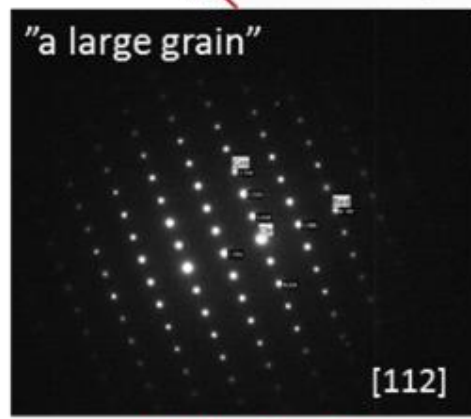
FCC austenite

Results

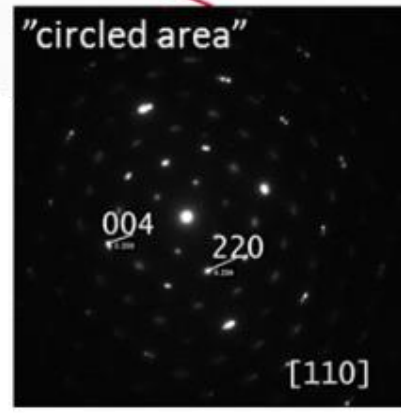
Compositions and crystal structures (100 dpa)



$Ni_{0.4-0.7}Fe_{1.3-1.7}Cr_{0.8-1.3}O_4$



$Ni_{0.8}Fe_{1.2}Cr_{1.0}O_4$



Outer layer
 $Ni_{0.8}Fe_{1.2}CrO_4$ grains

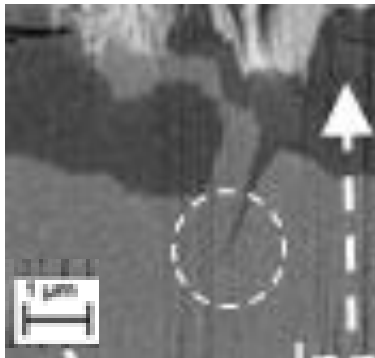
Inner layer
 $Ni_{0.7}FeCr_{1.3}O_4$
Epitaxial

Results

Common features (0, 50 and 100 dpa samples)

- Oxide intrusion at the inner oxide/metal substrate boundaries

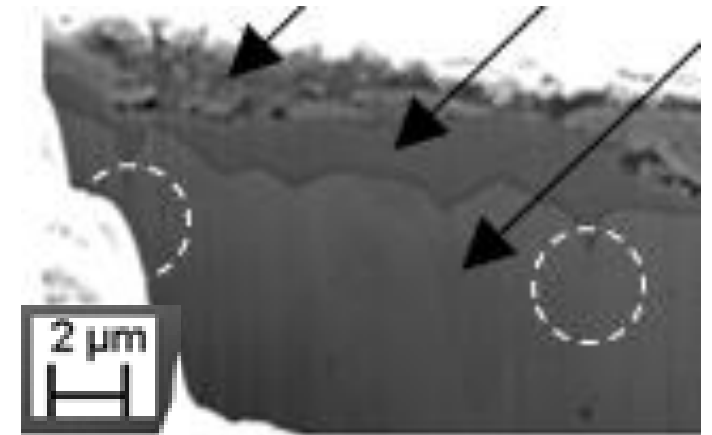
0 dpa



50 dpa



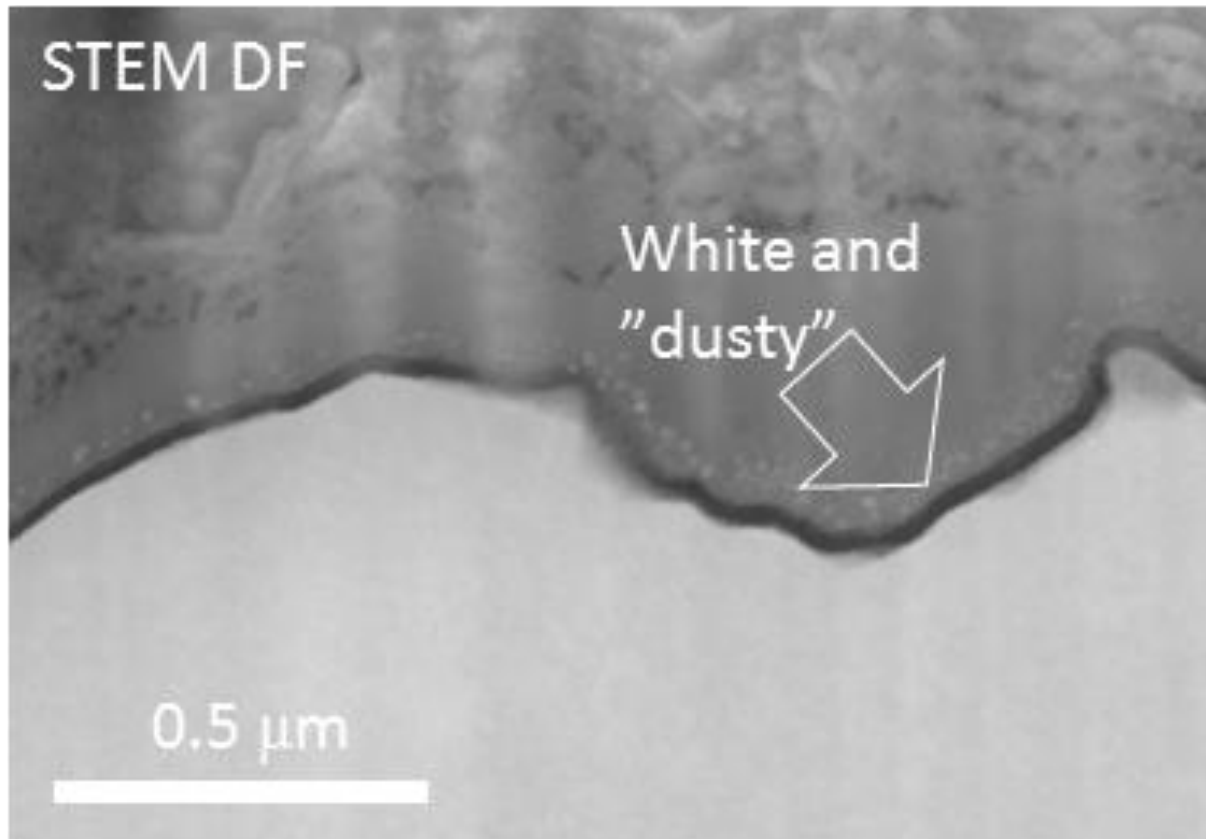
100 dpa



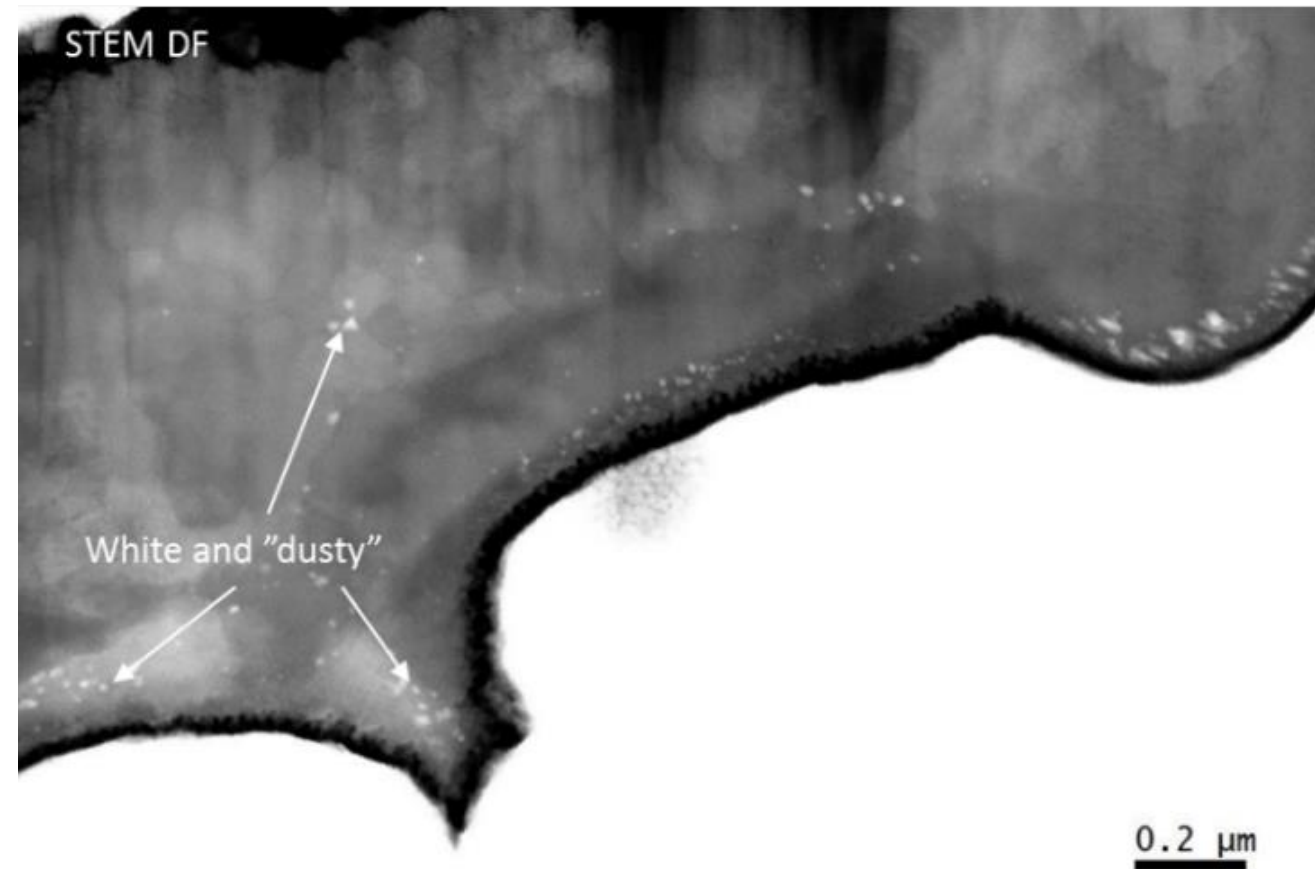
Results

Common features (50 and 100 dpa samples)

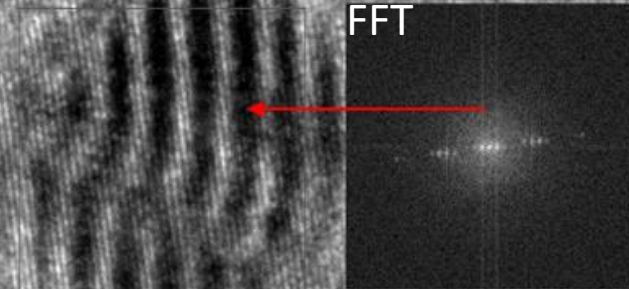
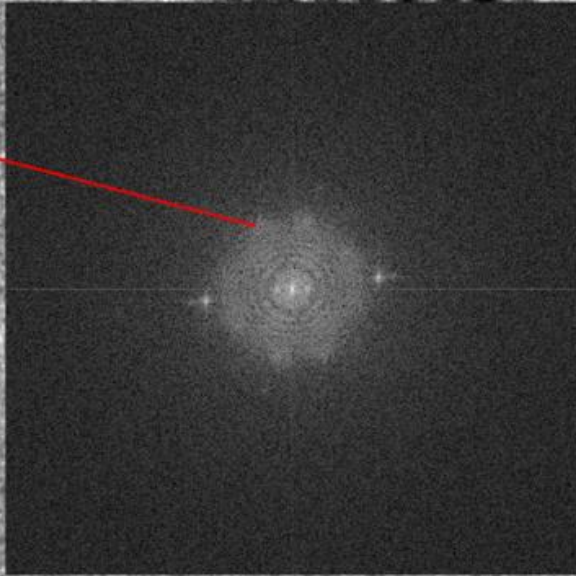
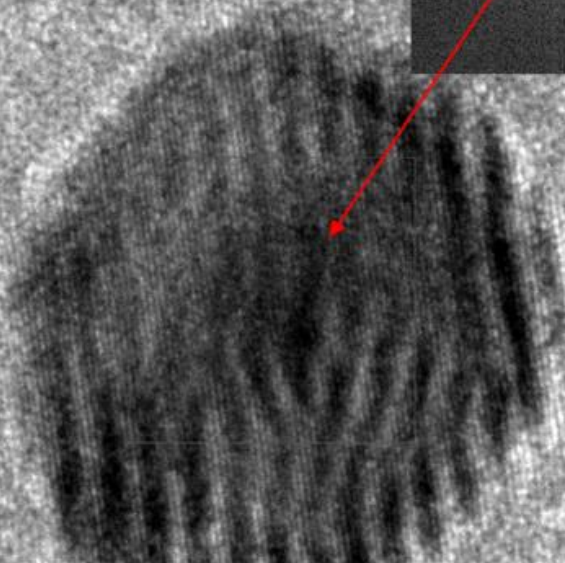
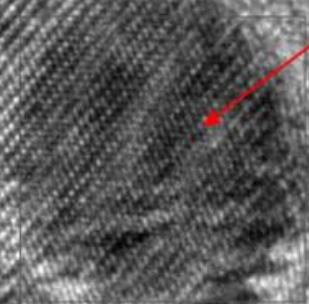
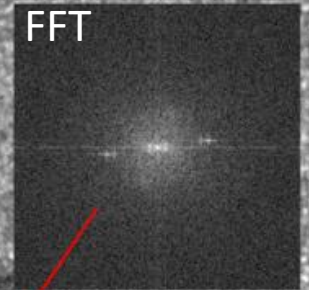
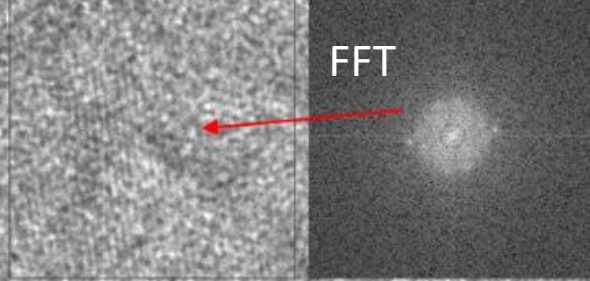
50 dpa



100 dpa



HRTEM



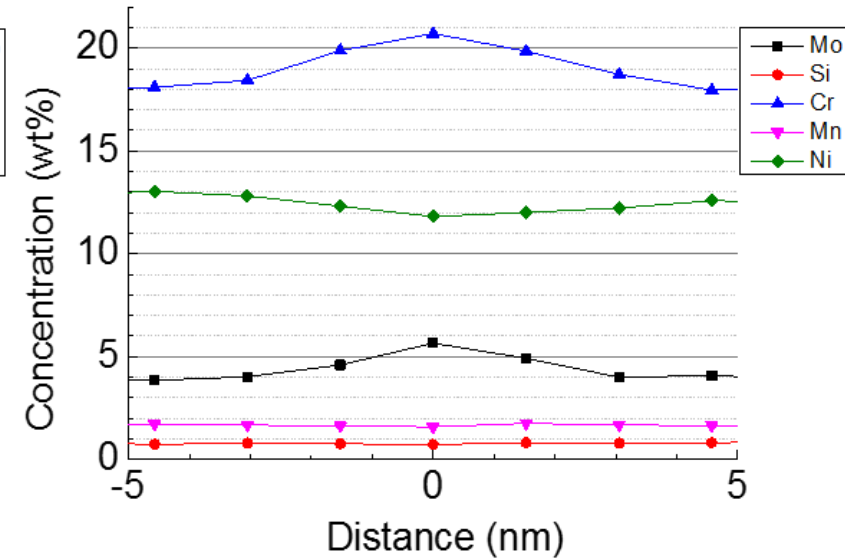
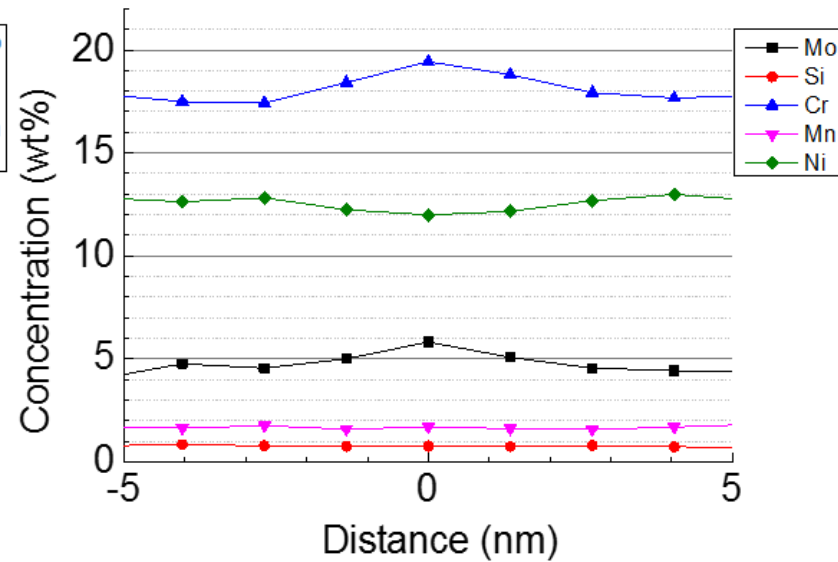
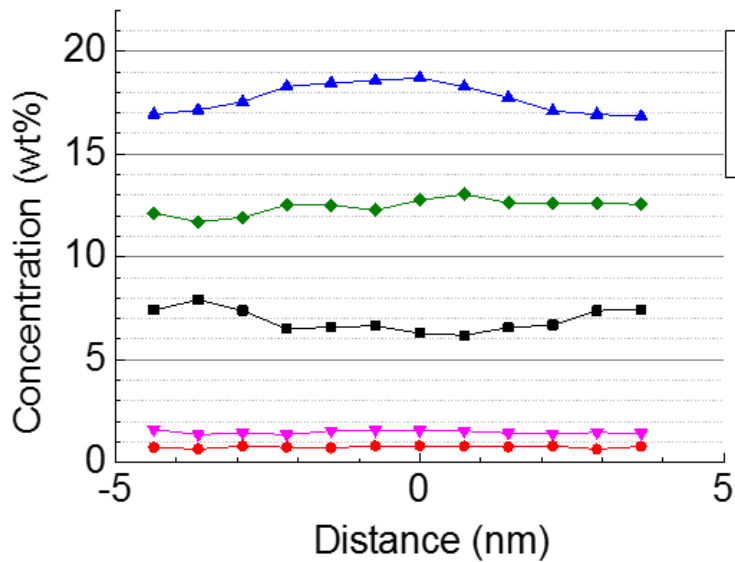
5 nm

A white horizontal scale bar representing 5 nm.

Results

G.B. compn of metal/metal near oxide films

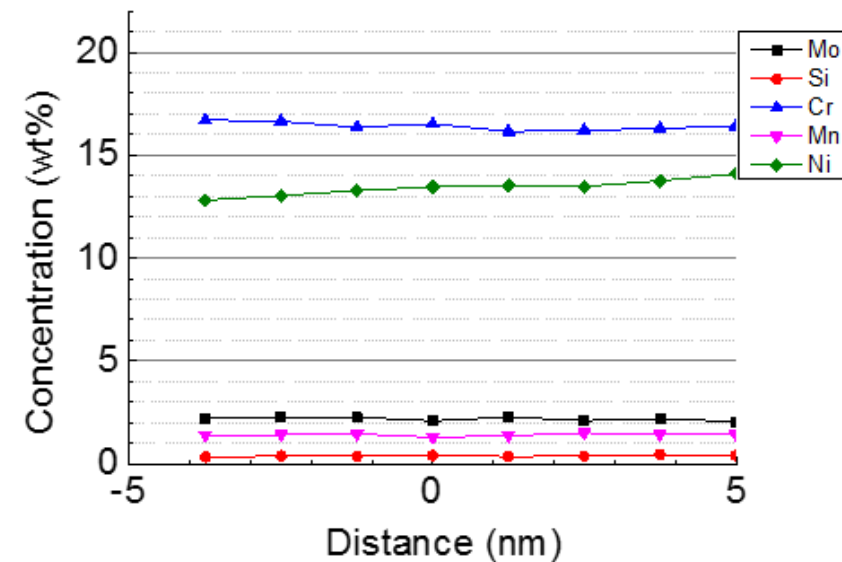
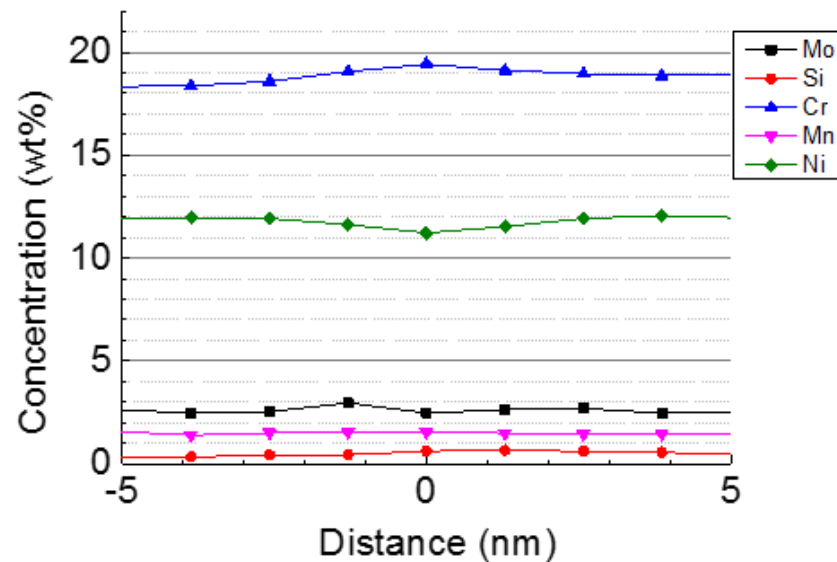
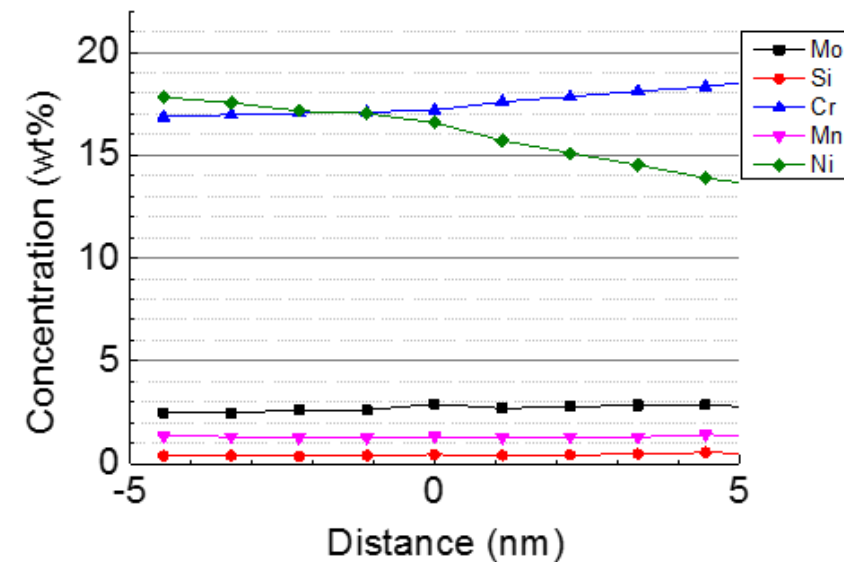
0 dpa sample



Results

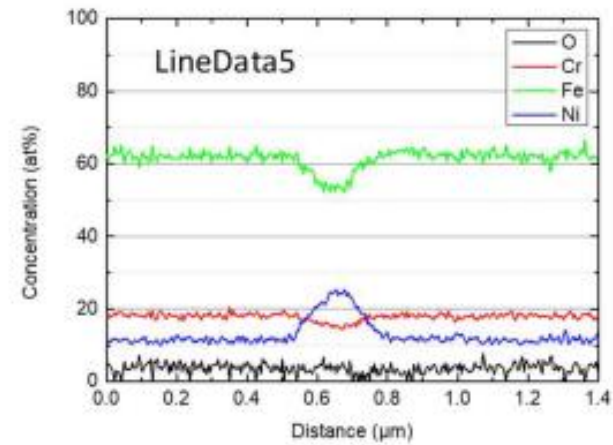
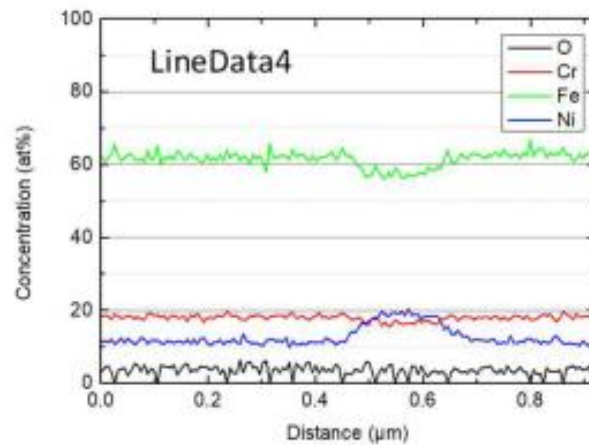
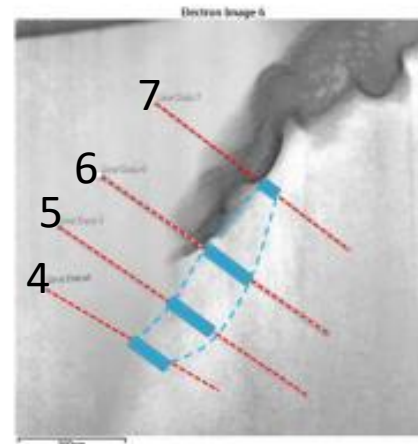
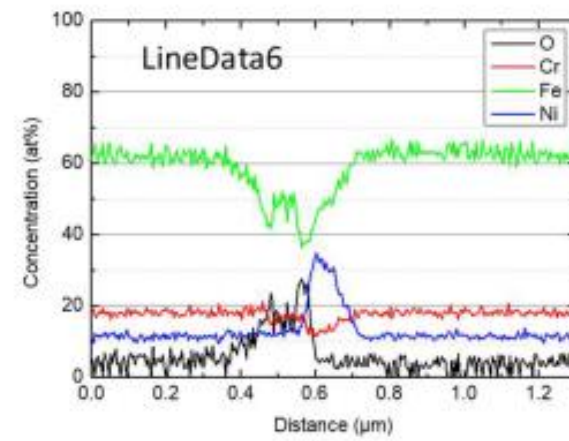
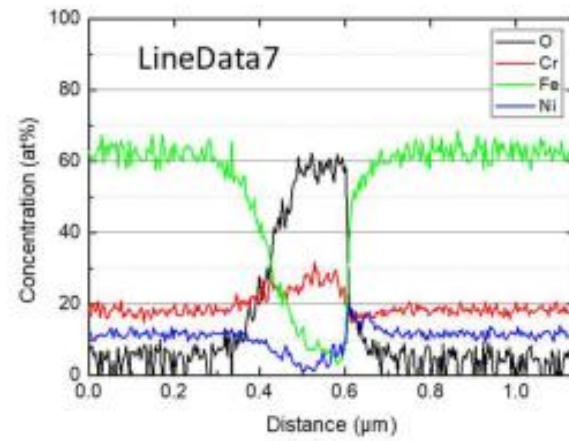
G.B. compn of metal/metal near oxide films

50 dpa sample



Results

100 dpa sampl



Note:

$$W_m = W_L + W_i$$

Metal weight consumed by corrosion (W_m) = Test coupon weight change (W_L) + Weight of oxides on the test coupon surface (W_i)

$$\frac{1}{\rho_m A} \frac{\Delta W_m}{\Delta \tau} : \text{Metal thinning rate } (\rho_m: \text{metal density, } A: \text{test coupon surface area})$$

$$\frac{1}{\rho_{ox} A} \frac{\Delta W_i}{\Delta \tau} : \text{Oxide growth rate } (\rho_{ox}: \text{oxides density})$$

Conclusions

- At all three dose levels, oxide penetration was observed at some metal/metal grain boundaries.
 - However, the penetration depth was only about 1-2 μm .
- All oxide films consisted of a duplex layer structure
 - an outer porous layer of fine spinel grains and an inner dense layer of epitaxially grown spinel.
- For the TEM-lamella “0_dpa” slight chromium enrichment was detected at the metal/metal grain boundaries near the oxide film, whereas for the TEM-lamella “50_dpa” no such enrichment or depletion could be clearly identified.
- The present study has not provided any evidence of irradiation enhanced corrosion of the stainless steel material.

Acknowledgements

- Mr. Michael Jacobsson and Dr. Johan Öijerholm at Studsvik Nuclear AB are thanked for preparing small samples for FIB/SEM. Mr. Daniel Jädernäs (Studsvik Nuclear AB) and Dr. Fredrik Gustavsson (Swerea KIMAB, Sweden) prepared the TEM-lamellae for this examination.
- Scientific discussion as offered by Dr. Mattias Thuvander and Dr. Kristina Lindgren (Chalmers University of Technology, Sweden) and Ms. Jenny Roudén (Ringhals AB) are gratefully acknowledged.
- The irradiated material for this study was used with permission of Ringhals AB.
- Sample preparation was funded by Electric Power Research Institute (USA) while the TEM examination was performed under contract with the Swedish Radiation Safety Authority.